Research Article

Melatonin modifies tumor hypoxia and metabolism by inhibiting HIF-1α and energy metabolic pathway in the *in vitro* and *in vivo* models of breast cancer

André de Lima Mota[1], Bruna Victorasso Jardim-Perassi[1], Tialfi Bergamin de Castro[2], Jucimara Colombo[1], Nathália Martins Sonehara[1], Victor Keniti Gomes Nishiyama[1], Vinicius Augusto Gonçalves Pierri[1], Debora Aparecida Pires de Campos Zuccari*[1,2]

[1]Laboratory of Molecular Investigation of Cancer – LIMC, Faculdade de Medicina de São José do Rio Preto/FAMERP, São José do Rio Preto, Brazil
[2]Universidade Estadual Paulista "Júlio de Mesquita Filho" – UNESP, São José do Rio Preto, Brazil
*Correspondance: debora.zuccari@famerp.br; Tel: +55 (17) 3201-5700 / +55 (17) 3201-5928, Fax: +55 (17) 3229-1777

Running title: Melatonin and tumor hypoxia in breast cancer

Received: October 2, 2019; Accepted: December 4, 2019

ABSTRACT

Breast cancer is the most common cancer among women and has a high mortality rate. Adverse conditions in the tumor microenvironment, such as hypoxia and acidosis, may exert selective pressure on the tumor, selecting subpopulations of tumor cells with advantages for survival in this environment. In this context, therapeutic agents that can modify these conditions, and consequently the intratumoral heterogeneity need to be explored. Melatonin, in addition to its physiological effects, exhibits important anti-tumor actions which may associate with modification of hypoxia and Warburg effect. In this study, we have evaluated the action of melatonin on tumor growth and tumor metabolism by different markers of hypoxia and glucose metabolism (HIF-1α, glucose transporters GLUT1 and GLUT3 and carbonic anhydrases CA-IX and CA-XII) in triple negative breast cancer model. In an *in vitro* study, gene and protein expressions of these markers were evaluated by quantitative real-time PCR and immunocytochemistry, respectively. The effects of melatonin were also tested in a MDA-MB-231 xenograft animal model. Results showed that melatonin treatment reduced the viability of MDA-MB-231 cells and tumor growth in Balb/c nude mice ($p < 0.05$). The treatment significantly decreased HIF-1α gene and protein expression concomitantly with the expression of GLUT1, GLUT3, CA-IX and CA-XII ($p < 0.05$). These results strongly suggest that melatonin down-regulates HIF-1α expression and regulates glucose metabolism in breast tumor cells, therefore, regulating hypoxia and tumor progression.

Keywords: Breast cancer, hypoxia, intratumoral heterogeneity, melatonin, HIF-1α, tumor microenvironment.

1. INTRODUCTION

Breast cancer is the second most prevalent neoplasia in the world, the most common type of tumor among women, and the fifth largest cancer-related cause of death (1). About 40% of

breast tumors have hypoxic regions, which have been associated with an increased metastasis, higher relapse rate, and a reduced rate of survival (2, 3). When tumors reach about 1-2 mm, their metabolic demands become restricted due to limited diffusion of oxygen and nutrients (4). The low O_2 levels characterize the hypoxia, which results in uncontrolled cell proliferation, fast tumor growth and consequent inadequate perfusion (5, 6).

Intratumoral hypoxia is considered as a marker of poor prognosis in cancer patients and is associated with resistance to chemotherapy and radiotherapy, promotion of angiogenesis, tumor cells invasion and metastasis (7, 8). Effects of hypoxia in tumor cells are multifaceted, which may promote apoptosis and necrosis, or induce the expression of a large number of genes, leading to cellular adaptation and survival under adverse conditions imposed by the tumor microenvironment. Hypoxia, acidosis and oxidative stress are examples of conditions that may exert selective pressure during tumor evolution, forcing "natural selection" of subpopulations within the tumor, characterizing the intratumoral heterogeneity (9). These tumor cell subpopulations show different phenotypes based on aggressiveness and sensitivity to treatment (10).

HIF-1 is the main component in the cellular response to hypoxia. It is a heterodimeric transcription factor with two subunits, HIF-1α and HIF-1β (9). Under physiological conditions, HIF-1β is constitutively expressed and HIF-1α is maintained at low level (11). In hypoxia, tumor cells overexpress HIF-1α, which regulates the expressions of several genes, including those involved in glucose metabolism and angiogenesis (12). Therefore, HIF-1α overexpressed in tumor hypoxic regions can be used as a marker of tissue oxygenation levels (13). Another important marker of hypoxic areas is pimonidazole (14, 15), a nitroimidazole, its reduced form binds to peptides containing the thiol group (- SH). Its reduction is dependent on pO_2, since O_2 competes with pimonidazole for the addition of electrons in the molecule itself. Therefore, low O_2 regions are favorable for the reduction of pimonidazole (16, 17).

In hypoxic intratumoral areas, an adaptive mechanism consists in the high expression of the glucose transporter 1 (GLUT-1), leading to increased glucose uptake (18), which contributes to increased anaerobic glycolysis rather than oxidative phosphorylation (Warburg effect) by tumor cells (19, 20). GLUT-3 also has higher expression in tumor tissues, especially in breast cancer. However, the increase of its expression is less frequent when compared to GLUT-1 (21). Studies suggest that these transporters are positively regulated by HIF-1α and overexpressed in hypoxic tumors (21, 22). The high expression of GLUT-1 and GLUT-3 are related to high proliferation rates, low differentiation, breast tumors with high histologic grade and estrogen receptor (ER) and progesterone (PR) negative status (23, 24). These glucose receptors have been explored in antitumor therapies, and their low expression is associated with reduced tumor growth (24, 25).

In response to low vascularization and the Warburg effect, there is an increase in lactate production and hydrogen ions, which are then exported to the extracellular space, acidifying the tumor microenvironment (26). Naturally, the low pH induces apoptosis in normal cells, which does not occur in tumor cells. Instead, the acid pH seems to confer advantages to tumor cells (27). In this context, carbonic anhydrases (CA) play an important role in the CO_2 transport and in the control of intracellular pH. CA-IX and CA-XII are hydrogen ions carrier proteins that contribute to the transport of lactate through interactions with monocarboxylate transporter (MCT). CAs are fundamental components in the homeostasis of the intracellular pH and therefore in the acidification of the extracellular space (28, 29). In this context, intratumoral heterogeneity, hypoxia and acidosis constitute an obstacle to tumor therapy, and agents that can modify these adverse conditions in the tumor microenvironment must be explored (30).

Melatonin (N-acetyl-5-methoxytryptamine) has been noted as a possible treatment molecule against breast cancer. Melatonin is a hormone synthetized mainly by the pineal gland and its

production is inhibited in the presence of light (31, 32). Studies have reported that exogenous melatonin administration is effective in inhibiting the tumor growth *in vitro* and *in vivo* in different types of cancer (33). Many oncoprotective and oncostatic properties have been assigned to melatonin, and recent studies demonstrate the impact of circadian rhythm disruption on the Warburg effect (34). It has been reported that exposure to light at night induces a constant stimulation of tumor growth, since melatonin production is diminished. Exposure to light at night deregulates the circadian rhythm, which consequently disrupts tumor balance in favor of its constant growth (35). The protective effects of melatonin against hypoxia are mainly suggested by inhibition of HIF-1α expression and some of its target genes (36, 37). This molecule appears to inactivate the HIF-1α and to reduce the glycolysis or Warburg effect on cells highly dependent on this pathway, such as Ewing's sarcoma cells (38).

Thus, this study investigated the effects of melatonin treatment on different markers of hypoxia and glucose metabolism (pimonidazole, HIF-1α, GLUT1, GLUT3 and carbonic anhydrases IX and XII) in an experimental model of triple-negative breast cancer in the *in vivo* and *in vitro* conditions.

2. MATERIALS AND METHODS

2.1. Ethical Considerations.

This study was approved by the Ethics Committee on the Use of Animals of the Faculdade de Medicina de São José do Rio Preto (Prot. 001-003336 / 2014 - License CEUA 06/2014). The study was carried out following the national and international standards of ethics in animal experimentation.

2.2. Cell culture.

Triple negative human breast cancer cell line (MDA-MB-231) (ATCC, Manassas, VA, USA) was cultured with Dulbecco's modified Eagle's medium (DMEM) (GIBCO, Grand Island, NY, USA) supplemented with 10% of fetal bovine serum (FBS) (GIBCO, Grand Island, NY, USA), penicillin (100 IU/mL) and streptomycin (100 mg/mL) (GIBCO, Grand Island, NY, USA). For the *in vitro* study, the cells were divided into two groups: Melatonin treated group (1 mM, as was performed in a previous study (39) and control group treated with vehicle (0.5% ethanol).

2.2. Immunocytochemistry for cultured cells.

Immunocytochemistry was performed to evaluate the protein expression of HIF-1α, GLUT-1, GLUT-3, CA-IX and CA-XII markers after treatment with melatonin. The information and dilutions for each antibody are shown in Table 1.

Cells were trypsinized, re-suspended and seeded in silicone-plates adhered to silanized slides at 0.6 x 10^6 cells per well. After treatment, the medium was removed and cells were washed with phosphate buffered saline (PBS). Slides were incubated with 1 ml of 4% formaldehyde (Sigma-Aldrich) for 20 min to fixation. Subsequently, the silicones were uncoupled from the slides, which were incubated with 10% of H_2O_2 for 30 minutes to block endogenous peroxidase activity. Antigen exposure was performed in Triton solution (0.3%). Cells were washed with PBS between each step. Slides were incubated with the specific primary antibody (Table 1) in a dark wet chamber for 18 hours at 4 °C. Subsequently, they were washed with PBS for 15 minutes and incubated with the REVEAL - Biotin - Free Polyvalent DAB-HRP Kit (Spring Bioscience, USA) for 20 min and streptavidin -peroxidase

complex for 10 min. Slides were revealed using DAB chromogen at 0.5 % for 2-5 minutes (DAB, Signet® Covance Laboratories, Dedham, MA, USA). The slides were counterstained with hematoxylin for 40 seconds. The reactions were accompanied by a positive control for the primary antibody and negative control.

Slides were observed on the 40X objective of the Nikon Eclipse E200 microscope and analyzed by optical densitometry. For each sample, three different fields were photographed and the immunoreactive areas were quantified by measuring the pixels intensity in 20 points using *ImageJ Software* (NIH, Bethesda, MD, USA), totaling 60 points quantified for each slide. The values were obtained as arbitrary units (au) and the mean optical density (MOD) showed the staining intensity specifically in the immunoreactive areas.

Table 1: Antibodies information and different dilutions used for immunostaining.

Antibody	Company	Code	Dilution
HIF-1α	Santa Cruz	H1alpha67	1:50
GLUT-1	Abcam	Ab115830	1:1200
GLUT-3	Sigma	6515	1:400
CA-IX	Sigma	2D3	1:1000
CA-IXX	Sigma	CLO280	1:400

2.3. Gene expression by quantitative real-Time PCR (qPCR).

qPCR was performed to evaluate the gene expression of HIF-1α, GLUT-1 and CA-XII after treatment with melatonin (1 mM). Cells were seeded in a 6-wells plate (10-cm^2 each) at 0.5 x 10^6 cells per well and separated into treated and control groups. The treatments were performed for 24 hours. Total RNA was extracted from the cells using Trizol reagent (Invitrogen Life Technologies – Eugene, OR, USA), as the manufacturer recommends. The RNA concentration of each sample was determined with NanoDrop2000 (Thermo Fisher Scientific, Rockford, IL, USA). The RNA from each sample was reverse-transcribed to complementary DNA (cDNA) using a High Capacity cDNA kit (Applied Biosystems, Foster City, CA, USA). First, the standard curve was calculated, and analyzed for the differential expression of HIF-1αor GLUT-1 or CA-XII and endogenous control ACTB was performed using SystemStepOnePlus (Applied Biosystems, Foster City, CA, USA) and TaqMan Universal Master Mix (Applied Biosystems, Foster City, CA, USA). The assays used were HIF-1α (Hs00153153_m1), GLUT-1 (Hs00892681_m1), CA-XII (Hs01080902_m1) and ACTB (Hs99999903_m1) (Applied Biosystems, Foster City, CA, USA). Each reaction consisted of 10 µL of Master Mix, 1 µL of TaqMan, 8 µL of DEPC water and 1 µL of cDNA (100 ng/mL). The qPCR conditions were 95°C for 10 minutes followed by 40 cycles of 95°C for 15 seconds and 60°C for 1 minute. The expression of each gene was calculated relative to the normalized expression of gene used as endogenous control (ΔΔCt). The samples were tested in triplicate, and all experiments included the negative control.

2.4. Animal model.

Female Balb/c nude athymic mice were purchased from São Paulo University Medical School (USP-SP) and were transported to Faculdade de Medicina de São José do Rio Preto (FAMERP). Mice were housed in pathogen free conditions at room temperature (21 to 25 ºC) under 12/12 h light/dark cycle. Food and water were offered *ad libitum.* MDA-MB-231 cells were injected in the right flank at $5x10^6$ in 50 µL of FBS-free medium.

2.5. Melatonin administration.

Mice were randomly assigned to either melatonin administration (n = 7) or control group (vehicle treated, n = 7). Vehicle solution was prepared with 8 ml of phosphate buffered saline (PBS), 1 ml of dimethyl sulfoxide (DMSO) and 1 ml of Cremophor (Sigma, St. Louise, MO, USA) and given in 100 μL of solution by intraperitoneal injection (IP). Melatonin (Sigma, St. Louise, MO, USA) was diluted in vehicle, and mice received IP of 100 μL of melatonin containing solution (40 mg/kg of body weight as performed in a previous study (33). Melatonin was administered 1 hour before room lighting was switched off. Treatment started 10 days after tumor cells injection and continued for 14 days. IP injections were given 5 days a week.

Tumor size was measured weekly with caliper. Length and width values were recorded and tumor volume was calculated using the formula: Length x $(Width)^2$ x 0.52.

After euthanasia, tumors were removed and divided into two pieces; one was used for immunohistochemistry and one for RNA extraction and further qPCR.

2.6. Immunohistochemistry for tumor tissue obtained from animals.

Immunohistochemistry was performed on the tumor tissue to evaluate the expression of HIF-1α, pimonidazole, GLUT-1, GLUT-3, CA-IX and CA-XII. The standard dilutions for each antibody are described in Table 1. For detection of pimonidazole, the kit (Hypoxyprobe ™-1 Omni Kit Inc., USA) was used. Pimonidazole was injected intraperitoneally at 60 mg/kg and mice euthanized one hour after injection. Then, tumors were removed, cut longitudinally and tissue was histologically processed. Histological sections of 4 μm were obtained from the paraffin embedded material. Subsequently, slides were deparaffinized in an incubator at 60 °C, followed by incubation in xylol and decreasing ethanol concentrations. Antigen retrieval was done in a cooker pan (ARNO, São Paulo, SP, Brazil) at 95 °C with citrate buffer (pH 6.0) for 30 min. After cooling, the slides were incubated with 3 % hydrogen peroxidase for 30 min to block endogenous peroxidase activity and the subsequent steps were performed as described in 2.2.

For pimonidazole, antigen exposure was performed in Triton solution (0.3%). Endogenous peroxidase blockade was performed in solution of methanol and hydrogen peroxide for 30 minutes. Histological slides were analyzed by optical densitometry as described in 2.3.

2.7. Gene expression by quantitative Real-Time PCR for tumor tissues.

Total RNA was extracted from the tumor fragments following the Trizol reagent protocol (Invitrogen®). Initially, tumor fragments were stored in polypropylene falcon tubes containing RNA stabilization solution (RNA later). Tumors were cut and each fragment, weighing 100 mg, was inserted into a falcon tube containing 1 mL of Trizol. The fragments were macerated using a macerator (Politron®), and another 1 ml of Trizol was added to the tube. Subsequently, 200 μL of chloroform were added to each 1 mL of Trizol, and kept at room temperature for 3 minutes. Tubes were centrifuged at 14,000 rcf for 20 minutes at 4 °C. The resulting aqueous phase was transferred to a new tube, and 400 μL of isopropyl alcohol were added for precipitation of the RNA followed by incubation at room temperature for 15 minutes. Then, it was centrifuged at 14,000 rcf for 20 minutes at 4°C, and RNA pellet was washed with 1 ml of 75% ethanol and centrifuged again at 7,500 rcf for 7 minutes at 4 °C. The supernatant was discarded and the pellet diluted in 30 μL of DEPC (diethyl pyrocarbonate) water (Invitrogen®).

To analyze the expression of HIF-1A, GLUT1 and CA-XII genes, cDNA synthesis with the reverse transcriptase enzyme and real time PCR were performed as described above in 2.3.

2.8. Statistical analysis.

For samples with normal distribution, the comparison of two parameters was performed by *Student t* test. For comparison of more than two parameters, we used the analysis of variance (ANOVA) followed by *Bonferroni's* test. P values <0.05 were considered significant and all analyses were performed using *Prism 6.0 software* (GraphPad, La Jolla, CA, USA).

3. RESULTS

3.1. Effects of melatonin on tumor growth *in vivo.*

The weight of the mice was monitored during the experiment, and neither melatonin therapy nor vehicle had any effect on the animal weights during the study period. Treatments started 10 days after tumor cell injection, and tumor volumes were measured weekly. Tumors reached large volume, especially in control group, with ulceration 24 days after tumor cell injection. Results showed that tumor growth was slower in the treated group than that in the control-group ($p < 0.05$; Figure 1A). Figure 1B shows a mouse from the control group with tumor volume of 878.8 mm^3 and a mouse of melatonin-treated group with tumor volume of 41.6 mm^3 (Figure 1C). One melatonin-treated mouse had tumor remission, showing a tumor of 18.72 mm^3 on day 7 which was not detected after 7 days of treatment. Tumor absence was confirmed in necropsy.

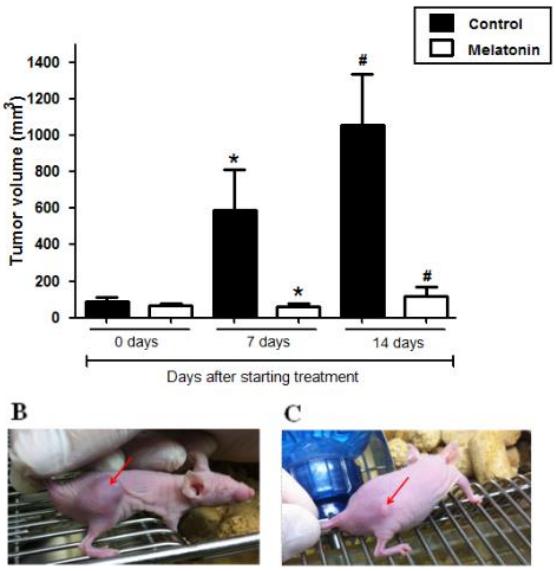

Fig. 1. Effects of melatonin on tumor growth in the Female Balb/c nude athymic mice.
*(A) Tumors volume were measured on days 0, 7 and 14 after start melatonin treatment (B) A representative mouse in control group. (C) A representative mouse in melatonin group. Data are expressed as mean ± SEM (n = 7). *p < 0.05 vs control after 7 days treatment. #p < 0.05 vs control after 14 days treatment. The red arrows indicate the tumors.*

3.2. Effects of melatonin on tumor HIF-1α expression at mRNA and protein levels in cultured cells.

In the *in vitro* study, qPCR was performed to analyze HIF1A gene expression in MDA-MB-231 cells treated with melatonin or vehicle (control). Results showed that melatonin treatment

for 24 hours was able to decrease the HIF1A gene expression compared with control group ($p = 0.0311$; Figure 2A). HIF-1α protein expression was also reduced by melatonin as verified by immunocytochemistry. However, the statistical significance level was not reached ($p > 0.05$; Figure 2B). The immunostaining for HIF-1α is shown in Figure 2C.

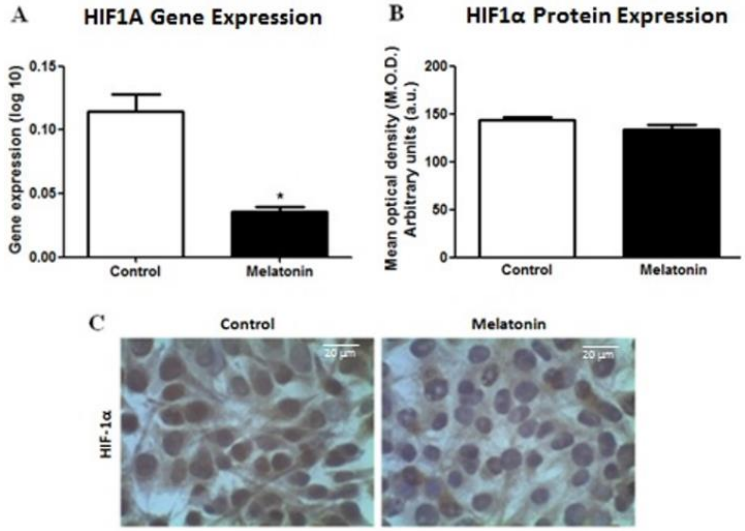

Fig. 2: Effects of melatonin on tumor HIF-1α gene expression in cultured cells.

(A) Statistical analysis of HIF1A gene expression (log 10). ***(B)*** *Statistical analysis of HIF-1α protein expression. (C) Representative images of immunostaining for HIF-1α. Data are expressed as mean ± SEM of 3 independent studies. 40X magnification, *p < 0.05 vs control.*

The results of HIF1A gene expression in tumor samples were showed in Figure 3A. In agreement with the *in vitro* study, a reduction of HIF1A gene expression was also observed *in vivo* in melatonin-treated mice ($p = 0.03$) and its reduction was more evident at protein levels ($p < 0.0001$; Figure 3B). The immunohistochemistry of HIF-1α in tumor samples is shown in Figure 3C.

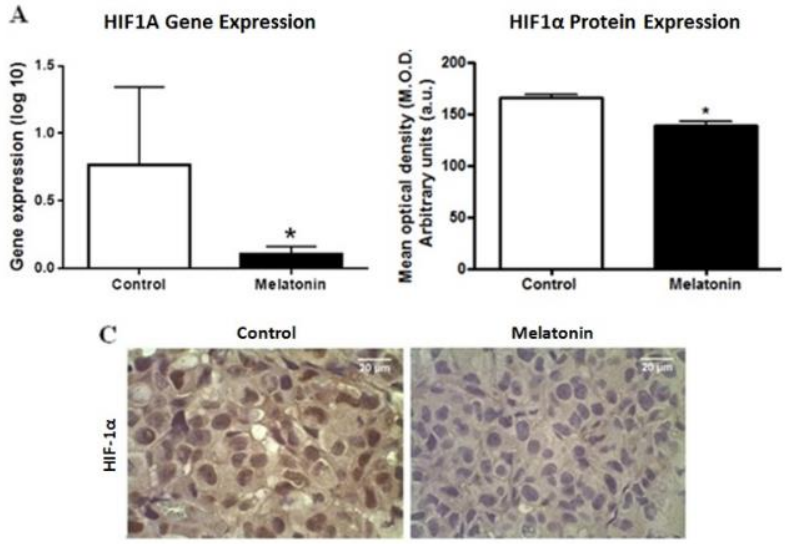

Fig. 3. Effects of melatonin on tumor HIF-1α expression in animal model,

*(A) Statistical analysis of HIF1A gene expression (log 10). (B) Statistical analysis of HIF-1α protein expression. Data are expression as mean ± SEM (n = 7). 40X magnification, *p < 0.05 vs control.*

3.3. Effects of melatonin on tumor hypoxia animal model.

Pimonidazole was used to analyze tumor hypoxia in mice treated with melatonin and vehicle (control). The immunostaining was observed predominantly in cytoplasm of tumor cells (Figure 4B). Results showed that melatonin was able to modify tumor hypoxia (Figure 4A). The quantitative analysis by densitometry showed that intensity of pimonidazole was significantly lower in melatonin-treated tumors than that in the control tumors ($p = 0.0033$; Figure 4A).

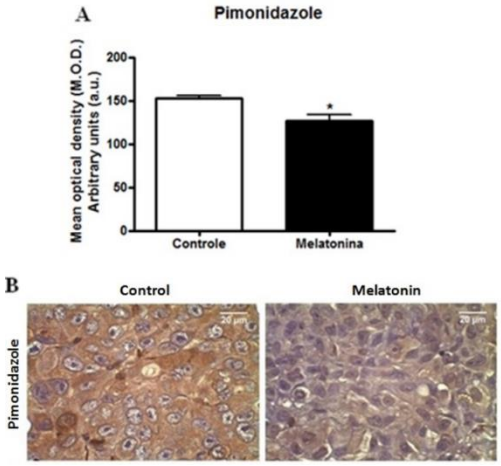

Fig. 4. Effects of melatonin on tumor hypoxia in animal model.

*(A) Statistical analysis of pimonidazole immunostaining. (B) Representative images of immunostaining for pimonidazole. Data are expressed as mean ± SEM (n = 7). 40X magnification, *p < 0.05 vs control.*

3.4. Effects of melatonin on glucose transporters (GLUT-1 and GLUT-3) and carbonic anhydrases (CA-IX and CA-XII) in the *in vitro* and *in vivo* studies.

Because HIF-1α can induce the expression of several genes under hypoxia, we tested the effects of melatonin on the HIF-1α targets genes, GLUTs and CAs. Melatonin significantly reduced gene expression of GLUT-1 ($p < 0.01$, Figure 5A) and CA-XII ($p < 0.01$, Figure 5B) in the cultured MDA-MB-231 cancer cells. However, quantifications of protein expression by optical densitometry for GLUT-1, GLUT-3, CA-IX and CA-XII in MDA-MB-231 did not show a significant difference between melatonin and control-groups ($p > 0.05$; Figure 6).

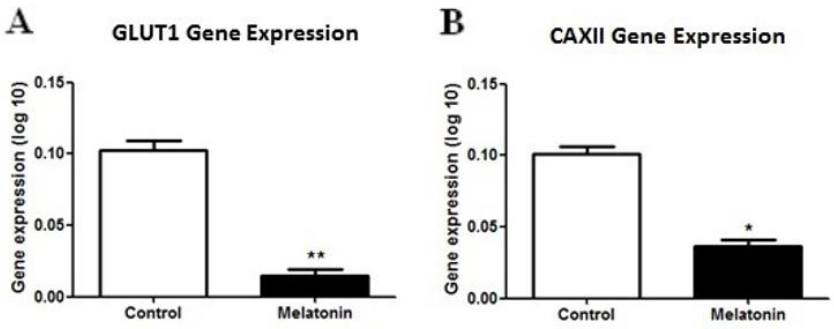

Fig. 5. Effects of melatonin on the gene expressions (mRNA) of GLUT1 and CAXII in MDA-MB-231 cancer cells.

*(A) Statistical analysis of GLUT1 and (B) CAXII gene expression (log 10). Data are expressed as mean ± SEM of 3 independent studies.*p < 0.01 vs control.*

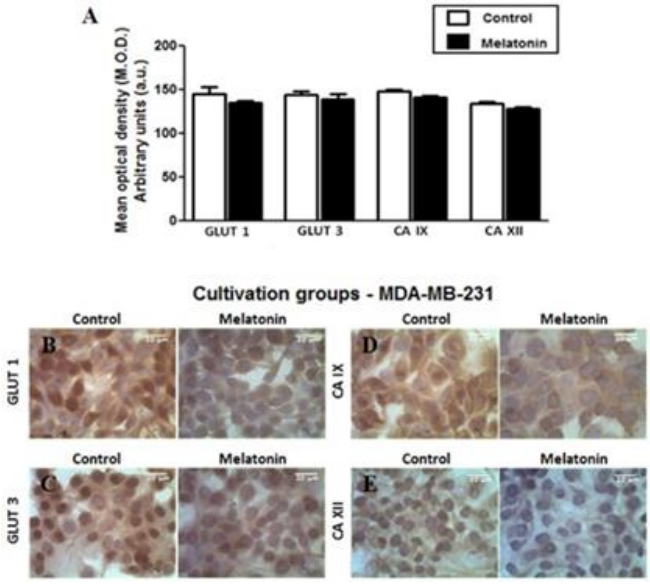

Fig. 6. Effects of melatonin on the protein levels of GLUT1, GLUT3, CA-IV and CAXII in MDA-MB-231 cancer cells.

(A) Statistical analysis of protein levels of GLUT-1, GLUT-3, CA-IX and CA-XII, respectively. Representative immunostaining images of (B) GLUT-1, (C) GLUT-3, (D) CA-IX and (E) CA-XII, respectively. No significant differences were detected between the treatments. Data are expression as mean ± SEM of 3 independent studies. 40X magnification.

In accordance with the *in vitro* results, in animal study, melatonin-treatment significantly downregulated gene expression (mRNA) of GLUT1 and CAXII in the tumors compared to the vehicle treated controls ($p < 0.01$; Figure 7A and B). In different from cultured cancer cells, the protein levels of LUT-1, GLUT-3, CA-IX and CA-XII in the animal tumor samples are significantly reduced after melatonin treatment compared to the untreated controls ($p < 0.01$, Figure 8 A). In the in vivo study, the protein levels of these genes were highly uniformed with their mRNA expression**.** The subcellular distributions of these biomarkers have also be investigated. It was showed that GLUT-1, GLUT-3, CA-IX and CA-XII were strongly expressed in cytoplasm. In addition, GLUT-1 and CA-XII were also expressed in membrane. (Figure 8B-E).

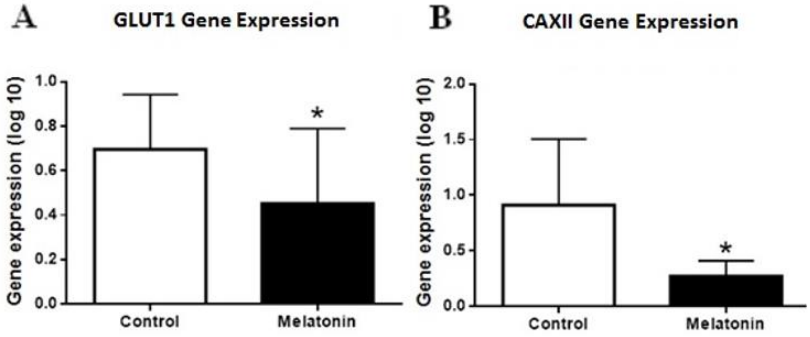

Fig. 7: Effects of melatonin on the gene expressions (mRNA) of GLUT1 and CAXII in tumors of animal study.

*(A) Statistical analysis of GLUT1 and (B) CAXII gene expression (log 10) in the tumors of animal study. Data are expressed as mean ± SEM (n = 7). *p < 0.05 vs control.*

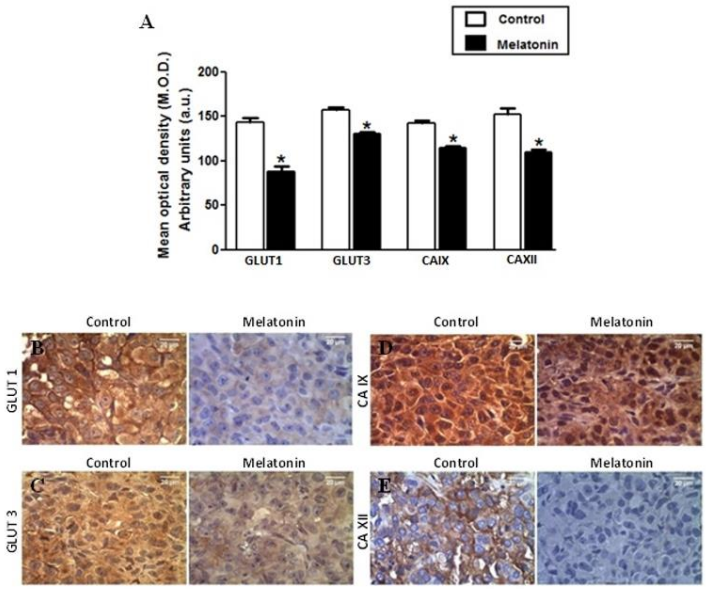

Fig. 8: Effects of melatonin on the protein levels of GLUT1, GLUT3, CA-IV and CAXII in tumors of animal study.

*(A) Statistical analysis of protein levels of GLUT-1, GLUT-3, CA-IX and CA-XII, respectively. Representative immunostaining images of (B) GLUT-1, (C) GLUT-3, (D) CA-IX and (E) CA-XII, respectively. Data are expression as mean ± SEM (n = 7). 40X magnification. * $p < 0.05$ vs control.*

4. DISCUSSION

In current study the results show that melatonin treatment modifies tumor hypoxia environment, downregulating the expression of HIF-1α at both of mRNA and protein levels in a mouse model of breast cancer. The inhibitory effect of melatonin on HIF-1 α gene expression is also confirmed in the *in vitro* study. These results are consistent with the previous reports which showed the inhibition of HIF-1α expression in different tumors with melatonin treatment (36, 37). In normoxia condition, HIF-1α is hydroxylated by prolyl hydroxylase domain (PHD) enzymes, the hydroxylyzed HIF-1α is then identified by von Hippel-Lindau protein (pVHL) and degraded by ubiquitin-proteasome system. In hypoxic conditions, the activities of PHDs are inhibited by the increased reactive oxygen species (ROS) leading to reduced HIF-1α hydroxylation and HIF-1α-pVHL binding. Thus HIF-1α degradation is blocked and its level is significantly elevated in hypoxia (40). Park *et al*. (41) have suggested that melatonin is able to restore HIF-1α-pVHL binding in tumor cells under hypoxia by normalizing HIF-1α level via its antioxidant action. In the same study, the authors believe that this inhibition occurs only at the level of HIF-1α protein expression but does not affect its mRNA expression. The inhibitory effect of melatonin on HIF-1α protein expression in hypoxia has also been observed by others (36).

In the *in vitro* study, we found that melatonin significantly decreased HIF-1α mRNA expression, but not protein expression. In the *in vivo* study, both of mRNA and protein expressions of HIF-1α were significantly decreased by melatonin treatment. We noticed that the results of the *in vitro* study might be related to the treatment-time schedule (24 h). A 24 h melatonin treatment might not be sufficient to induce significant changes of HIF-1α protein expression since the protein expression is always lagged behand of mRNA expression. This notion is supported by the report of Sohn *et al*. (42). According to these authors, melatonin is able to enhance miRNA3195 and miRNA374b expression, which inhibits HIF-1α gene

expression (42). The pimonidazole staining is another marker of tissue hypoxia and its low staining is usually associated with decrease of HIF-1α expression. We have observed that melatonin treatment significantly reduces the pimonidazole staining in the tumors compared to the control group. The similar results were reported by Sorace et al. (43), they also observed a decrease in pimonidazole staining in hypoxic BT474 tumors treated with trastuzumab. Thus, these results further suggest that melatonin has the capacity to reduce intratumoral hypoxia.

In hypoxic conditions, HIF-1α regulates several genes in order to promote the cellular adaptation to adverse conditions. These include glucose transporters. HIF-1α upregulates GLUT-1 and GLUT-3 in tumor cells, to increase their glucose uptake (24) which benefits the glycolysis. The process of glycolysis is predominant in hypoxia tumor cells (44) and these tumor cells primarily depend on this pathway to generate energy under hypoxic conditions (44, 45). Inhibition of HIF-1α expression is responsible for suppression of glycolytic activity in majority of cancers by affecting tumor adaptive mechanisms. Park *et al*. (46) have demonstrated that inhibition of HIF-1α intracellular pathways reduces the hypoxia-induced GLUT-1 and GLUT-3 expressions in adipose-derived stem cells (ASCs). Our results have showed that melatonin treatment also downregulates the expressions of GLUT-1 and GLUT-3 in mammary tumors at the gene or protein level, respectively. The inhibitory effect of melatonin on GLUT-1 is also verified in the cultured tumor cell line. The effects of melatonin on GLUTs expression are well documented (47). For example, Hevia *et al.* (48) have reported that melatonin competes with glucose to bind to GLUT-1 to decrease the glucose uptake and GLUT-1 expression in prostate cancer cells. The authors have also suggested that melatonin can be transported by GLUT-1, to increase its intracellular level.

GLUT-3 is also expressed in tumor tissue, but is less extensive than that of GLUT-1 (49). Many studies show that GLUT-3 expression is associated with aggressiveness and poor prognosis in gastric tumors, squamous oropharyngeal carcinoma and gliomas (50, 51). Actually, both GLUT-1 and GLUT-3 expressions are associated with tumorigenesis, cellular proliferation and lower survival rates in different types of cancer (52) and suppression of their expressions in intratumoral hypoxia areas contributes to a decrease in the glycolytic activity of tumor cells (53). Melatonin significantly suppresses the expressions of both of them in the breast cancer animal model or in the cancer cell line observed in the current study.

In intratumoral areas of hypoxia, CA-IX and CA-XII contribute to intracellular pH homeostasis through the transporting of hydrogen ions and lactate to the extracellular environment. Thus, these enzymes provide adaptive and survival mechanisms to tumor cells (54, 55). Recently, a CA-IX knockdown study shows that this enzyme contributes to tumor cell proliferation in the *in vitro* and *in vivo* conditions with its role in regulating the intracellular pH (56). Interestingly, CA-IX knockdown induces the CA-XII upregulation in colon tumor cells, showing a compensating mechanism between these two enzymes for regulation of pH beneficial to cancer cell proliferation and survival (56). Sowa *et al*. (57) have demonstrated that high HIF-1α and CA-IX expressions induce chemoresistance under hypoxia, and their inhibitions re-establish chemo sensibility in lung carcinoma cells. These results suggest that HIF-1α and CA-IX inhibitions improve prognosis in lung cancer patients with chemotherapy.

In accordance with these results we observed that, melatonin inhibited CA-IX and CA-XII expression in mammary tumors in the *in vivo* and *in vitro* conditions. Few studies have investigated the associations between melatonin and expressions of CA-IX and CA-XII (58, 59). Thus, the exact mechanisms are still unknown (60). Here we suggest that melatonin inhibits the activities of CA-IX and CA-XII by downregulation of HIF-1α expression in triple negative breast cancer model. It seems that the inhibitory effect of melatonin on CA-XII expression is more potent than that it is on CA-IX. High CA-XII expression in hypoxia conditions is observed in MCF-10A breast cell line. While high CA-IX and CA-XII expressions were concomitant with high pimonidazole staining in hypoxic areas of tumor

subjacent to necrosis in MDA-MB-231 xenograft tumors (60). Inhibition of CA-IX significantly reduces the invasive capacity of MDA-MB-231 tumor cell line in hypoxic conditions (61). CA-IX is considered as an independent prognosis marker which is clinically useful in predicting tumor progression, invasion and metastasis in breast cancer (62).

Collectively, in this study, we have observed that melatonin has the capacity to modify the tumor hypoxia environment by downregulation of HIF-1α gene expression in the *in vivo and in vitro* conditions. It seems that the suppression of melatonin on HIF-1α gene expression is more potent in the *in vivo* than that in the *in vitro*. These differences may relate to the variable microenvironments. The tumor microenvironment including immune cells (for example *in vivo*) is extremely important for their response to the treatment. Jardim-Perassi *et al*. (33) have showed that melatonin treatment reduces tumor growth in MDA-MB-231 breast cancer xenograft model with the modifications of gene expression associated with immune system in the tumor microenvironment. There are, at least, 57 differentially expressed genes mainly involved in immune response and all of these changes represent the tumor microenvironment. In addition, melatonin significantly suppresses the process of glycolysis by inhibiting GLUT-1, GLUT-3, CA-IX and CA-XII activities. These also help to improve the tumor microenvironment to further suppress the tumor growth. Taken together, our results suggest that melatonin can reverse adverse conditions in the tumor microenvironment to modify hypoxia and tumor progression.

ACKNOWLEDGEMENT

Grant support: Fundação de Amparo à Pesquisa do Estado de São Paulo (FAPESP 2014/25022-0).

AUTHORSHIP

DAPCZ conceived the study, designed the experiments and drafted the manuscript. ALM, BVJP, TBC, NMS, VKGN and VAGP carried out the in vitro and in vitro experiments, immunocytochemistry, immunohistochemistry and q-PCR. JC assisted in the analyses of data and with the production of the manuscript. All authors read and approved the final manuscript.

CONFLICT OF INTERESTS

The authors declare no conflate of interest, financial or other-wise.

Abbreviations

CA	Carbonic anhydrases
CAIX	Carbonic anhydrase 9
CAXII	Carbonic anhydrase 12
CO2	Carbon dioxide
GLUT1	Glucose transporter 1
GLUT3	Glucose transporter 3
HIF-1α	Hypoxia-inducible factor 1-alpha
MCT	Monocarboxylate transporter
MT1	Melatonin receptor 1
MT2	Melatonin receptor 2
O2	Oxygen
PHD	Prolyl hydroxylase domain

pO2	Partial oxygen pressure
pVHL	Von Hippel-Lindau
RE	Estrogen receptor
ROS	Reactive oxygen species
RP	Progesterone receptor

ORCID:

Tialfi Bergamin de Castro: number: 0000-0001-5366-7229
Debora Ap Pires de Campos Zuccari: ORCID number: 000-0002-0146-9041
Bruna Victorasso Jardim-Perassi: ORCID number: 0000-0001-5366-7229
Jucimara Colombo: ORCID number: 0000-0003-2183-9828

REFERENCES

1. Bray F, *et al.* (2018) Global cancer statistics 2018: GLOBOCAN estimates of incidence and mortality worldwide for 36 cancers in 185 countries. *CA. Cancer J. Clin.* **68**: 394-424 .
2. Flamant L, Notte A, Ninane N, Raes M, Michiels C (2010) Anti-apoptotic role of HIF-1 and AP-1 in paclitaxel exposed breast cancer cells under hypoxia. *Mol. Cancer* **9**: 19-28.
3. Guerrab A El, *et al.* (2017) Quantification of hypoxia-related gene expression as a potential approach for clinical outcome prediction in breast cancer. *PLoS One* **12**: e0175960.
4. Carmeliet P, Jain R K (2011), Molecular mechanisms and clinical applications of angiogenesis. *Nature* **473**: 298–307.
5. Vordermark D (2010) Hypoxia-specific targets in cancer therapy: Role of splice variants. *BMC Med.* **8**: 45.
6. Gilkes D (2016), Implications of Hypoxia in Breast Cancer Metastasis to Bone. *Int. J. Mol. Sci.* **17**: pii: E1669.
7. Manoochehri Khoshinani H, Afshar S, Najafi R (2016), Hypoxia: A Double-Edged Sword in Cancer Therapy. *Cancer Invest.* **34:** 536–545.
8. Chen C, Lou T (2017) Hypoxia inducible factors in hepatocellular carcinoma. *Oncotarget* **8**: 46691–46703.
9. Karakashev S V, Reginato M J (2015) Progress toward overcoming hypoxia-induced resistance to solid tumor therapy. *Cancer Manag. Res.* **7:** 253–764.
10. Hu Z, Sun R, Curtis C (2017) A population genetics perspective on the determinants of intra-tumor heterogeneity. *Biochim. Biophys. Acta - Rev. Cancer* **1867**: 109–126.
11. Semenza G L (2019) Pharmacologic Targeting of Hypoxia-Inducible Factors. *Annu. Rev. Pharmacol. Toxicol.* **59**, 379–403 (2019).
12. Ke Q, Costa M (2006) Hypoxia-Inducible Factor-1 (HIF-1). *Mol. Pharmacol.* **70**: 1469–1480.
13. Soni S, Padwad Y S (2017) HIF-1 in cancer therapy: two decade long story of a transcription factor. *Acta Oncol. (Madr).* **56**: 503–515.
14. Gabellieri C, Eykyn T R, Leach M O (2007) Conformational exchange in pimonidazole - a hypoxia marker. *Magn. Reson. Chem.* **45**: 621–623.
15. Ow C P C, Ullah M M, Ngo J P, Sayakkarage A, Evans R G (2019) Detection of cellular hypoxia by pimonidazole adduct immunohistochemistry in kidney disease: methodological pitfalls and their solution. *Am. J. Physiol. Physiol.* **317**: F322–F332.
16. Busk M, *et al.* (2013) PET imaging of tumor hypoxia using 18 F-labeled pimonidazole.

Acta Oncol. (Madr). **52**: 1300–1307.
17. Mascini N E, *et al.* (2016) Mass Spectrometry Imaging of the Hypoxia Marker Pimonidazole in a Breast Tumor Model. *Anal. Chem.* **88**: 3107–3114.
18. Lu Z L *et al.* (2019) Construction of a GLUT-1 and HIF-1α gene knockout cell model in HEp-2 cells using the CRISPR/Cas9 technique. *Cancer Manag. Res.* **11**: 2087–2096.
19. Pan H, Xia X, Pan H (2012) Active autophagy in the tumor microenvironment: A novel mechanism for cancer metastasis (Review). *Oncol. Lett.* **5**: 411–416.
20. Shi Y, Liu S, Ahmad S, Gao Q (2018) Targeting Key Transporters in Tumor Glycolysis as a Novel Anticancer Strategy. *Curr. Top. Med. Chem.* **18**: 454–466.
21. Chen X, *et al.* (2017) Predictive value of glucose transporter-1 and glucose transporter-3 for survival of cancer patients: A meta-analysis. *Oncotarget* **8**: 13206–13213.
22. Park H S, *et al.* (2016) Hypoxia induces glucose uptake and metabolism of adipose-derived stem cells. *Mol. Med. Rep.* **14**: 4706–4714.
23. Pinheiro C, *et al.* (2011) GLUT1 and CAIX expression profiles in breast cancer correlate with adverse prognostic factors and MCT1 overexpression. *Histol. Histopathol.* **26**: 1279–1286.
24. Ancey P B, Contat C, Meylan E (2018) Glucose transporters in cancer – from tumor cells to the tumor microenvironment. *FEBS J.* **285**: 2926–2943.
25. Madunić I V, Madunić J, Breljak D, Karaica D, Sabolić I (2018) Sodium-glucose cotransporters: New targets of cancer therapy? *Arh. Hig. Rada Toksikol.* **69**: 278–285.
26 Schawartz L, Supuran C T, Alfrouk K O (2017) The Warburg Effect and the hallmarks of Cancer. *Anticancer Agents Med. Chem.***17**: 164-170.
27. Paškevičiūtė M, Petrikaitė V (2019) Overcoming transporter-mediated multidrug resistance in cancer: failures and achievements of the last decades. *Drug Deliv. Transl. Res.* **9**: 379–393.
28. Chiche J, *et al.* (2009) Hypoxia-Inducible Carbonic Anhydrase IX and XII Promote Tumor Cell Growth by Counteracting Acidosis through the Regulation of the Intracellular pH. *Cancer Res.* **69**: 358–368.
29. Mboge M Y, *et al.* (2019) A non-catalytic function of carbonic anhydrase IX contributes to the glycolytic phenotype and pH regulation in human breast cancer cells. *Biochem. J.* **476**: 1497–1513.
30. Qian J, Rankin E B (2019) Hypoxia-induced phenotypes that mediate tumor heterogeneity. *Adv. Med. Biology*, **1135**, 43-55.
31. Reiter R J, *et al.* (2017) Melatonin, a full service anti-cancer agent: Inhibition of initiation, progression and metastasis. *Int. J. Mol. Sci.* **18**: pii: E843.
32. S. Bhattacharya S,, Patel K K, Dehari D, Agrawal A K, Singh S (2019) Melatonin and its ubiquitous anticancer effects. *Mol. Cell. Biochem.* https:/doi.org/10.1007/s11010-019-03617-5.
33. Jardim-Perassi B V, *et al.* (2019) RNA-Seq transcriptome analysis shows anti-tumor actions of melatonin in a breast cancer xenograft model. *Sci. Rep.* **9:** 966.
34. Proietti S, Cucina A, Minini M, Bizzarri M (2017) Melatonin, mitochondria, and the cancer cell. *Cell. Mol. Life Sci.* **74**: 4015–4025.
35. Moradkhani F (2019) Immunoregulatory role of melatonin in cancer. *J. Cell. Physiol* https:/doi.org/10.1002/jcp.29036.
36. Colombo J, Maciel J M W, Ferreira L C, da Silva R F, Zuccari D A P de C (2016) Effects of melatonin on HIF-1α and VEGF expression and on the invasive properties of hepatocarcinoma cells. *Oncol. Lett.* **12**: 231–237.
37. Al-Rasheed N M, *et al.* (2017) Original research paper. Pulmonary prophylactic impact of melatonin and/or quercetin: A novel therapy for inflammatory hypoxic stress in rats. *Acta Pharm.* **67**: 125-135.

38. Sanchez-Sanchez A M, *et al.*(2015) Melatonin cytotoxicity is associated to Warburg effect inhibition in Ewing sarcoma cells. *PLoS One* **1**0: e0135420 .
39. Jardim-Perassi B V, *et al.* (2014) Effect of melatonin on tumor growth and angiogenesis in xenograft model of breast cancer. *PLoS One* **9**: e85311.
40. Vriend J, Reiter R J (2016) Melatonin and the von Hippel-Lindau/HIF-1 oxygen sensing mechanism: A review. *Biochim. Biophys. Acta* **1865**: 176-183.
41. Park J W, Hwang M S, Suh S I, Baek W K (2009) Melatonin down-regulates HIF-1 alpha expression through inhibition of protein translation in prostate cancer cells. *J. Pineal Res.* **46**: 415–421.
42. Sohn E J, Won G, Lee J, Lee S, Kim S H (2015) Upregulation of miRNA3195 and miRNA374b Mediates the Anti-Angiogenic Properties of Melatonin in Hypoxic PC-3 Prostate Cancer Cells. *J. Cancer* **6**: 19-28.
43. Sorace A G, *et al.* (2017) Quantitative [(18)F]FMISO PET Imaging Shows Reduction of Hypoxia Following Trastuzumab in a Murine Model of HER2+ Breast Cancer. *Mol. Imaging Biol.* **19**: 130-137.
44. Liverani C *et al.* (2019) A biomimetic 3D model of hypoxia-driven cancer progression. *Sci. Rep.* **9**: 12263.
45. Sanchez-Sanchez A M, *et al.* (2015) Melatonin Cytotoxicity is associated to Warburg Effect inhibition in Ewing Sarcoma cells. *PLoS One* **10**: e0135420.
46. Park H S, *et al.* (2016) Hypoxia induces glucose uptake and metabolism of adipose-derived stem cells. *Mol. Med. Rep.* **14**: 4706-4714.
47. Mayo J C, *et al.* (2018) Melatonin uptake by cells: An answer to its relationship with glucose? *Molecules* **23**: pii: E1999 .
48. Hevia D, *et al.* (2015) Melatonin uptake through glucose transporters: a new target for melatonin inhibition of cancer. *J. Pineal Res.* **58**, 234–250.
49. Kocdor, M A *et al.* (2013) Progressive increase of glucose transporter-3 (GLUT-3) expression in estrogen-induced breast carcinogenesis. *Clin. Transl. Oncol.* **15**: 55-64.
50. Liu Y, *et al.* (2009) The expression and significance of HIF-1alpha and GLUT-3 in glioma. *Brain Res.* **1304**, 149-54.
51. Schlößer H A, *et al.* (2017) Glucose transporters 1, 3, 6, and 10 are expressed in gastric cancer and glucose transporter 3 is associated with UICC stage and survival. *Gastric Cancer* **20**: 83–91.
52. Chen X, *et al.* (2017) Predictive value of glucose transporter-1 and glucose transporter-3 for survival of cancer patients: A meta-analysis. *Oncotarget* **8**: 13206-13213.
53. Labak C M, *et al.* (2016) Glucose transport: meeting the metabolic demands of cancer, and applications in glioblastoma treatment. *Am. J. Cancer Res.* **6**: 1599-608 (2016).
54. Jamali S, *et al.* (2015) Hypoxia-induced carbonic anhydrase IX facilitates lactate flux in human breast cancer cells by non-catalytic function. *Sci. Rep.* **5**: 13605.
55. Ames S, Pastorekova S, Becker H M (2018) The proteoglycan-like domain of carbonic anhydrase IX mediates non-catalytic facilitation of lactate transport in cancer cells. *Oncotarget* **9**: 27940-27957.
56. Parks S K, Cormerais Y, Durivault J, Pouyssegur J (2017) Genetic disruption of the pHi-regulating proteins Na+/H+ exchanger 1 (SLC9A1) and carbonic anhydrase 9 severely reduces growth of colon cancer cells. *Oncotarget* **8**: 10225-10237.
57. Sowa T, *et al.* (2017) Hypoxia-inducible factor 1 promotes chemoresistance of lung cancer by inducing carbonic anhydrase IX expression. *Cancer Med.* **6**: 288-297.
58. Crooke A, Huete-Toral F, Martínez-Águila A, Martín-Gil A, Pintor J (2012) Involvement of carbonic anhydrases in the ocular hypotensive effect of melatonin analogue 5-MCA-NAT. *J. Pineal Res.* **52**: 265-270.
59. Siddiqui M H, *et al.* (2019) Exogenous melatonin counteracts NaCl-induced damage by

regulating the antioxidant system, proline and carbohydrates metabolism in tomato seedlings. *Int. J. Mol. Sci.* **20**: pii: E353

60. Tafreshi NK, *et al.* (2016) Evaluation of CAIX and CAXII Expression in Breast Cancer at Varied O2 Levels: CAIX is the Superior Surrogate Imaging Biomarker of Tumor Hypoxia. *Mol. Imaging Biol.* **18**: 219-231.
61. Meehan J, *et al.* (2017) Inhibition of pH regulation as a therapeutic strategy in hypoxic human breast cancer cells. *Oncotarget* **8**: 42857-42875.
62. Chu C Y, *et al.* (2016) CA IX is upregulated in CoCl2-induced hypoxia and associated with cell invasive potential and a poor prognosis of breast cancer. *Int. J. Oncol.* **48**: 271-280.

Please cite this paper as:
Mota, A., Jardim-Perassi, B., de Castro, T., Colombo, J., Sonehara, N., Nishiyama, V., Pierri, V. and Zuccari, D. 2019. Melatonin modifies tumor hypoxia and metabolism by inhibiting HIF-1α and energy metabolic pathway in the in vitro and in vivo models of breast cancer. Melatonin Research. 2, 4 (Dec. 2019), 83-98. DOI:https://doi.org/https://doi.org/10.32794/mr11250042.